

Assessment of Human 2D and 3D Hepatic Co-culture Models and In Vitro to In Vivo Extrapolation Modeling as an Alternative Approach Method to Traditional Hepatotoxicity Testing

Sage Corzine ¹, Nimisha Bhattarai ¹, Marjory Moreau ¹ and Jamie B. Scaglione ^{1,*}

Final Report

January 2023

¹ScitoVation, 6 Davis Drive, Suite 146, Durham, NC 27709

*Address correspondence to:

Jamie Scaglione
6 Davis Drive
Suite 146
PO Box 13479
Durham, NC 27709
919 354-5219
jscaglione@scitovation.com

Abstract

Many chemicals possess potential for liver toxicity. In fact, the liver is the most common target tissue among regulated compounds in various chemical databases. Historically, the chemical and pharmaceutical industries have relied on data from in vivo animal studies to understand the safety of chemicals and drugs and to obtain regulatory approval for intended uses. However, given the Environmental Protection Agency's (EPA) September 10, 2019, memo committing to the end of mammal in-life testing by 2035, development of systems that faithfully capture human liver toxicity is a major focus of both academic and industrial research. Here we report the characterization of 2D and 3D human hepatic mono- and co-culture models utilizing liver sinusoidal endothelial cells (LSECs) and hepatic stellate cells (HSCs). We tested the models with a diverse 12 compound panel, ranging from known pharmaceutical hepatotoxins to environmental contaminants to assess cytotoxic response. In Vitro to In Vivo Extrapolation (IVIVE) modeling was used to predict in vivo human equivalent dose compared to LC50 in vitro exposure concentration. We have found that inclusion of LSECs and HSCs results in a model with higher reproducibility but see few differences in cytotoxic effects between 2D and 3D culture models.

Introduction

The liver is responsible for a wide range of functions, including xenobiotic detoxification, synthesis and storage of glucose, production of the bile necessary for digestion, protein synthesis, and regulation of blood cholesterol and triglycerides. The liver parenchymal cells, hepatocytes, possess high capacity for biotransformation of a variety of chemicals, making the liver an important determinant of the effect and toxicity of a chemical in the body. Many chemicals, including many commodity chemicals, possess potential for liver toxicity. In fact, the liver is the most common target tissue in rodents among regulated compounds in various chemical databases.¹ The chemical and pharmaceutical industries have historically relied on data from *in vivo* animal studies to understand the safety of chemicals and drugs and to obtain regulatory approval for intended uses. However, significant interspecies differences in structure, isoforms, expression, and catalytic activity of liver enzymes result in poor concordance between animal and human toxicity.^{2,3} Therefore, development of systems that more faithfully capture human liver toxicity is a major focus of both academic and industrial research.

The chemical industry could benefit greatly from the application of human-based *in vitro* liver models to reduce its reliance on high-dose animal studies for risk determination. However, there is a noted gap in development and validation of hepatotoxicity models using non-pharmaceutical compounds. In contrast, extensive efforts in the pharmaceutical industry are underway to develop and validate various *in vitro* liver models for accurate and reliable prediction of drug-induced liver injury (DILI) in early stages of drug development.^{4,5} DILI is a major reason for the termination of promising drug development projects. Thorough assessment of potential liver toxicity at the preclinical drug development stage is essential to prevent potential safety liabilities and to reduce the risk of expensive late-stage product failures. Analogously, a tiered approach to commodity chemical safety testing—in which more efficient and species-relevant *in vitro* alternatives are applied during the early stages of chemical product development—would reduce the need for *in vivo* animal studies and speed up chemical development and regulatory approval while lowering costs and risk.

In vitro 2D and 3D liver models range in complexity from isolated perfused rat models, precision-cut liver slices, isolated human hepatocytes, hepatoma cell lines, organoid cell culture and “organ on a chip”.⁶ Hepatoma cell lines express only very low levels of metabolizing enzymes, while primary human hepatocytes (PHHs) are considered the gold standard cell model for predictive toxicology due to their ability to reflect the complete functionality of the human organ *in vivo*.^{7,8} However, 2D PHH cultures have been criticized due to their absence of *in vivo*-like cellular density and their cellular homogeneity – lacking hepatic stellate cells (HSCs), Kupffer cells and liver sinusoidal endothelial cells (LSECs).⁹ Furthermore, 2D PHH cultures can rapidly dedifferentiate losing hepatic functions.¹⁰ 3D liver organoids have been reported to be a superior, more physiologically relevant model for liver toxicity compared to 2D. However, these systems can be technically challenging and are low throughput.

To directly compare the functional utility of these models, we established, evaluated and characterized 2D and 3D human hepatic mono- and co-culture models utilizing liver sinusoidal endothelial cells (LSECs) and hepatic stellate cells (HSCs). We tested the models with a diverse 12 compound panel, ranging from known pharmaceutical hepatotoxins to environmental contaminants to assess cytotoxic response. We used these data and IVIVE to compare the *in vitro* apical measures of cellular health status to predicted concentrations *in vivo*. We have found that inclusion of LSECs and HSCs with

PHHs results in a model with higher reproducibility, but we see few differences in cytotoxic effects between 2D and 3D culture models.

Materials and Methods

Test compounds and concentrations

Chemicals used were purchased from Millipore Sigma (St. Louis, MO). Stock solutions were prepared in either DMSO or culture medium. Serial dilutions of drug solutions were prepared freshly before treatment. The concentration of each compound stock was at 1000x or 500x C_{max} or maximumly dissolvable in solvent at room temperature. The final concentration of DMSO in all treatment and control media did not exceed 0.2%. For compound treatment with liver spheroids, 2x of final concentrations were prepared for each compound's serial dilution. For spheroid culture in Perkin Elmer 96-well CellCarrier Spheroid ULA plates (Perkin Elmer Cat No. 6055330) each well contained 100 μ L medium. During treatment, 50 μ L medium was first removed from one well of the spheroid culture and the 50ul serial dilutions of 2x the final concentration of the testing compound was added to the spheroid culture to bring the total volume up to 100 μ L. The compounds and concentrations used are listed in Supplementary Table 1.

Cytotoxicity and viability

Fluorescence based cytotoxicity assays were performed on 2D cultures using the Celltox Green express kit from Promega (Catalog # G8731). The assay reagent was diluted 1:1000 into the treatment media and the wells were imaged by brightfield and fluorescence microscopy at multiple fields of view with a 20X/0.4NA dry objective and a FITC-compatible filter set on a PerkinElmer Opera Phenix High Content Screening System.

Bioluminescent-based ATP assays were performed using the Celltiter-Glo Viability Assay kit from Promega (Catalog # G7572) with modified procedures for 2D or the Celltiter-Glo 3D Viability Assay kit from Promega (Catalog # G9683) for 3D. Briefly, the ATP assay began by removing all the media from each well of the 96 well plate then adding dPBS (100 μ L 2D, 50 μ L 3D) and an equivalent volume of assay reagent to each well. The rest of the assay was performed according to manufacturer's instructions and measured on a Molecular Devices FlexStation 3 plate reader for analysis.

Bioluminescent-based LDH assays were performed using the LDH-Glo Cytotoxicity Assay from Promega (Catalog# J2381) on 3D culture media diluted 1:50 in LDH storage buffer. The assay performed according to manufacturer's instructions and measured on a Molecular Devices FlexStation 3 plate reader for analysis.

2D PHH Mono and co-culture

Cryopreserved human hepatocytes from a single individual obtained from Lonza or CellzDirect were thawed per the vendors' instructions in hepatocyte thawing media (MCAT50, Lonza). The cells were centrifuged at 100 g for 8 min and resuspended in hepatocyte plating media (MP100, Lonza). Viable cells were counted manually using a hemocytometer by Trypan Blue exclusion method.

Cryopreserved human-derived liver sinusoidal endothelial cells (LSECs) and hepatic stellate cells (HSCs) obtained from Lonza were thawed per the vendors' instructions. LSECs and HSCs were centrifuged at 150 g for 5 min, and pellets were resuspended in the appropriate volume of DMEM+ 20% FBS media. Viable cells were counted manually using a hemocytometer by Trypan Blue exclusion method. Prior to their use for plating co-cultures, LSECs and HSCs were grown and maintained in collagen-coated flasks.

For 2D models, hepatocytes alone (mono-cultures) or hepatocytes, LSECs and HSCs together (co-cultures) were seeded on collagen-coated Perkin Elmer Viewplates (Cat #6005182). For mono-cultures, 50,000 hepatocytes per well were seeded in hepatocyte plating media (MP100, Lonza). Co-cultures were plated in media containing equal volumes of hepatocyte plating media MP100 and DMEM+ media. For co-cultures, 50,000 hepatocytes + 4,000 LSECs + 4,000 HSCs were seeded per well of a 96-well plate. 4-6 h after plating the media was changed to maintenance media to remove dead cells. A complete media change using maintenance media (50/50 HCM+/DMEM+) was performed every 24 h. Compound dosing was performed 48 h after plating as described above. Cytotoxicity and Viability assays were performed 24 h after dosing. The experimental design is outlined in Supplementary Figure 1.

3D PHH Mono and Co-culture

Cryopreserved spheroid verified human hepatocytes (CHHs) from a single individual were obtained from Lonza and thawed per the vendors' instructions in hepatocyte thawing media (MCAT50, Lonza). The cells were centrifuged at 100 g for 8 min and resuspended in hepatocyte plating media (MP100, Lonza). Viable cells were counted manually using a hemocytometer by Trypan Blue exclusion method.

Cryopreserved human-derived liver sinusoidal endothelial cells (LSECs) and hepatic stellate cells (HSCs) obtained from Lonza were thawed per the vendors' instructions. LSECs and HSCs were centrifuged at 150 g for 5 min, and pellets were resuspended in the appropriate volume of DMEM+ 20% FBS media. Viable cells were counted manually using a hemocytometer by Trypan Blue exclusion method. Prior to their use for plating co-cultures, LSECs and HSCs were grown and maintained in collagen-coated flasks.

For 3D models, hepatocytes alone (mono-cultures) or hepatocytes, LSECs and HSCs together (co-cultures) were seeded on Perkin Elmer CellCarrier Spheroid ULA plates. For mono-cultures, 2000 hepatocytes per well were seeded in 20% FBS spheroid formation media plating media. For co-cultures, 2000 hepatocytes + 500 LSECs + 500 HSCs were seeded per well of a 96-well plate in the same media. A half medium change using maintenance media (50/50 HCM+/DMEM+) was performed after 96 h. Compound dosing was performed 7 d after plating as described above. Cytotoxicity and Viability assays were performed 72 h after dosing. The experimental design is depicted in Supplementary Figure 2. The composition of all media used for 2D and 3D culture is outlined in Supplementary Table 2.

2D monolayer culture composition

To assess the overall composition of the 2D cultures, a variety of fluorescent cell dyes were used. The NPCs were stained with Celltracker dyes (LSECs with Celltracker Green and HSCs with Celltracker Orange) diluted 1:1000 in media for 45 minutes before plating. The cells were plated in mono-culture (HSC, LSEC and hepatocytes) or in co-culture and then maintained for 72 h as described in the previous section. They were imaged with the Opera Phenix High Content imager, then stained with Hoechst and imaged again.

For gene expression analysis, cells were seeded as above. At 72 h, RNA was extracted from mono- and co-culture cells using RNeasy Mini Kit (Qiagen) according to manufacturer's protocol. For first-strand cDNA synthesis, 1 µg of total RNA was extended to 20 µl total reaction volume containing 10 µl of 2X RT buffer mix by using the High-Capacity RNA-to-cDNA™ kit (Applied Biosystems) according to manufacturer's protocol. All primers were purchased from Integrated DNA Technologies (Morrisville, NC). Quantitative reverse-transcriptase polymerase reactions were performed using the Fast SYBR™ Green Master mix (Applied Biosystems, Thermo Fisher Scientific). The RT-PCR assays were performed in duplicate using a 7900HT Fast Real-Time PCR system (Applied Biosystems). The amplified PCR products were quantified by calculating the cycle thresholds (CTs) for the individual target gene and normalizing to three housekeeping genes, GAPDH, β-actin and 18s RNA. The sequences of all primers used are in Supplementary Table 3. Analysis was done using the $\Delta\Delta C_t$ method.¹¹

Spheroid morphology and composition

To further characterize 3D mono and co-cultures, live spheroids were stained with 5-carboxyfluorescein diacetate (5-CFDA, 5 µM) in 50/50 media (HCM + DMEM) for 1 h to visualize formation of bile canaliculi and imaged using the 20X/0.4NA dry objective on a PerkinElmer Opera Phenix High Content Screening System. The Celltracker experiment was also repeated in 3D cultures. The 2 NPC types were stained with different Celltracker dyes as described above before plating the co-culture and then imaged after 72 hours using the 20X water objective on a PerkinElmer Opera Phenix High Content Screening System.

For immunofluorescence staining, the mono and co-culture spheroids were fixed with 4% paraformaldehyde at 4°C overnight, followed by permeabilization with 0.2% TritonX at 4°C overnight. Spheroids were blocked with 3% BSA diluted in PBS for 2 h at RT. Subsequently spheroids were stained with primary antibodies (Albumin anti-mouse (Abcam **ab106582**), HNF α anti-chicken (Abcam **ab41898**), CYP3A4 anti-mouse (Santa Cruz sc-53850), ACTA anti-rabbit (Abcam **ab124964**), LYVE1 anti-rabbit (Invitrogen PA1-16635), Cd68 anti-mouse (Abcam ab955)) at 4°C overnight. Finally, spheroids were stained with the respective secondary antibodies (Invitrogen Goat anti-Rabbit Alexa Fluor Plus™ 488 (A32731), Invitrogen Goat anti-Chicken Alexa Fluor™ 568 (A-11041), Invitrogen Goat anti-Mouse Alexa Fluor™ 568 (A-11004)) for 2 h at RT and imaged using 20X water objective on a PerkinElmer Opera Phenix High Content Screening System.

3D mono- and co-cultures were also functionally characterized using qPCR to evaluate gene expression of CYP3A4, LYVE1, ACTA, and albumin using GAPDH and β-actin as housekeeping genes. These targets were selected to provide markers of HSCs (ACTA), LSECs (LYVE1), hepatocytes (albumin) and drug metabolizing capability, as CYP3A4 is a primary drug metabolic enzyme. Briefly, 30 spheroids were harvested on days 0, 3, 7 and 10 and lysed mechanically. RNA was

then extracted using a Qiagen RNeasy Micro kit. Subsequently, cDNA was generated using Applied Biosystems High-Capacity RNA to cDNA kit and an Applied Biosystems Veriti 96 well Thermal Cycler. Finally, qPCR was performed for the genes mentioned above using an Applied Biosystem7900HT Fast Real-Time PCR System. Analysis was done using the $\Delta\Delta C_t$ method.¹¹

Determination of IC50 and EC50 values

GraphPad Prism was used to calculate IC50 (CellTiter-Glo) and EC50 (CellTox Green) values for compound dose–response relationships. A 4-parameter Hill function was fit to the normalized CellTiter-Glo Viability, Celltiter-Glo 3D viability and CellTox Green HCI dead cell count data by least squares regression with no weighting. A bottom constraint of 0% and a top constraint of 100% were included in the parameters.

Quantitative in vitro to in vivo extrapolation for 2D and 3D (QIVIVE)

IVIVE is a quantitative method that allows for the estimation of a concentration at which effects are observed. In vitro concentrations (AC50, BMDs or NOAEL/LAOEL) are used to calculate equivalent in vivo blood concentrations and then, by reverse dosimetry, in vivo exposures are estimated for use in the prioritization of chemicals for risk assessment¹. To determine the equivalent oral dose of exposure in human (HED) of the compounds tested above, a simple steady-state pharmacokinetic relationship was used to extrapolate the active concentration from in vitro assays.

Estimated equivalent oral doses for liver compounds were calculated from the liver toxicity assay results. First, the chemical steady-state blood concentrations (C_{ss}) were estimated as described in Wetmore et al. (2015).¹² The basic equation using generic parameters to calculate static C_{ss} is based on continuous uptake of a daily oral dose:

$$C_{ss} = \frac{Ko}{(GFR \times Fub) + \frac{Qh \times Fub \times CL_{int}}{Qh + Fub \times CL_{int}}} \quad (1)$$

Where, Ko = chemical exposure rate ($\mu\text{g}/\text{h}$); Qh = hepatic blood flow (90.97 L/h); Fub = unbound fraction of parent compound in the blood (EPA dashboard); CL_{int} = hepatic intrinsic metabolic clearance (EPA dashboard); GFR = glomerular filtration rate (7.68 L/h).

The model for C_{ss} is linear with respect to dose rate Ko , so C_{ss} was predicted for a dose rate of 1 mg/kg body weight/day which is 3333.33 $\mu\text{g}/\text{h}$ with a human average BW of 80kg.

We used In Vitro to In Vivo Scaling (IVIVS) to convert the in vitro CL_{int} ($\mu\text{L}/\text{min}/10^6$ cells) into in vivo CL_{int} (L/h).

$$CL_{int \text{ in vivo}} = \frac{CL_{int \text{ in vitro}} \times HPGL \times V \times 60}{1000} \quad (2)$$

Where, $CL_{int \text{ in vitro}}$ is the intrinsic clearance in $\mu\text{L}/\text{min}/10^6$ cells, $HPGL$ is the hepatocellularity (110×10^6 cells per g liver)³, V is the liver volume (1614g).

The oral Human Equivalent Dose (mg/kg/day) was also calculated as described in Wetmore et al. 2015:¹²

$$HED = POD (\mu M) \times \frac{1 \frac{mg}{kg}/day}{C_{SS} (\mu M)} \quad (3)$$

Results and Discussion

To assess the overall composition of the 2D cultures, a variety of fluorescent cell dyes were used. Live hepatocytes auto-fluoresce in the Hoechst channel and dead hepatocytes auto-fluoresce in the Celltracker Green channel (Figure 1A). This autofluorescence provides a viable method for imaging hepatocytes in 2D co-culture, as the NPCs (stained with Hoechst and Celltracker Green or Orange, Figures 1B and 1C) do not auto fluoresce in the Hoechst channel. We were therefore able to stain LSECs with Celltracker Green and HSCs with Celltracker Orange prior to seeding and utilize the hepatocyte autofluorescence to confirm the presence of all cell types (Figure 1D). After staining with Hoechst, the exposure time of the images is reduced and the autofluorescence of the hepatocytes becomes very dim in comparison (Figure 1E).

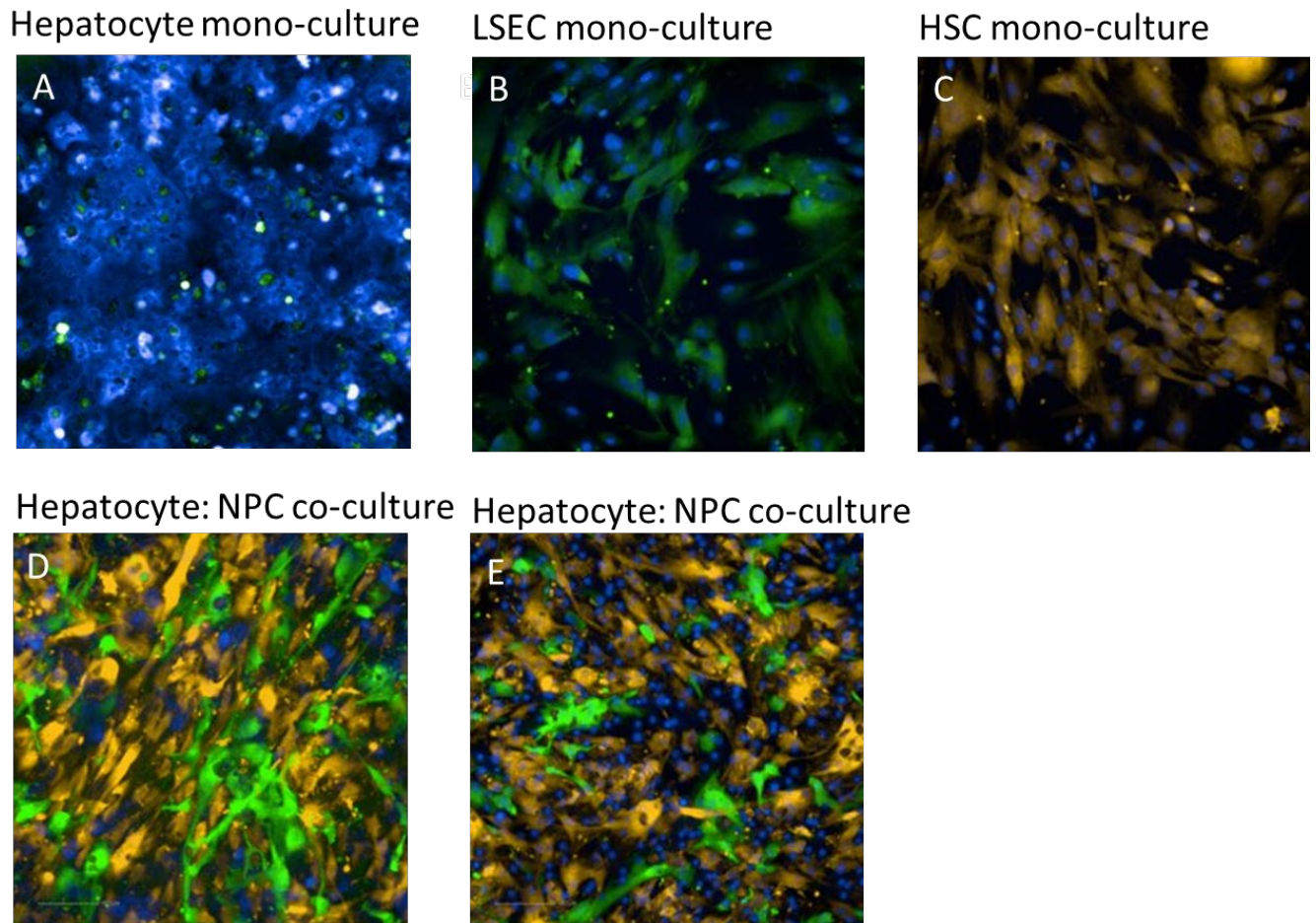


Figure 1: Representative fluorescent images of hepatocytes, LSEC and HSC alone (A, B, C, respectively) and hepatocytes NPCs (LSEC, HSC) in co-culture (D, E) after 72 h in HCM+/DMEM+ (50/50%) media. Panel A shows the autofluorescence of the live hepatocytes (blue) and the dead hepatocytes (green). Before Hoechst staining, (D) the live hepatocytes (blue), LSEC (green) and HSC (orange) are all visible. After Hoechst staining just before imaging, (B, C, E) the nuclei of all cell types are visible (blue) as well as the Celltracker dyes in the LSECs (green) and HSCs (orange) that were added prior to seeding.

To assess the overall composition of the 3D cultures, we used fluorescent cell dyes as well as immunostaining for cell type specific markers. Live hepatocytes auto-fluoresce in the Hoechst channel while the NPCs do not (Figure 1). This autofluorescence provides a viable method for imaging hepatocytes in 3D co-culture. We were therefore able to stain LSECs with Celltracker Green and HSCs with Celltracker Orange prior to seeding and utilize the hepatocyte autofluorescence to confirm the presence of all cell types (Figure 2C). From these images, it appears that both types of NPCs are present at the exterior of the co-culture spheroids, while the hepatocytes are concentrated toward the center. This is also supported by the staining images of the NPC and hepatocyte specific markers (Figures 4 and 5). The presence of the NPCs allows the co-culture spheroids to form after 3 days. At this time, the bile canalicular network can be visualized by staining with 5-CFDA (Figure 3). 5-CFDA is taken up by functional hepatocytes, hydrolyzed to the strongly fluorescent 5-carboxyfluorescein (5-CF) and secreted out of hepatocytes where it accumulates in bile canaliculi. In contrast, the mono-cultures are not fully formed until day 7 and no bile canaliculi are visible on day 3 (data not shown).

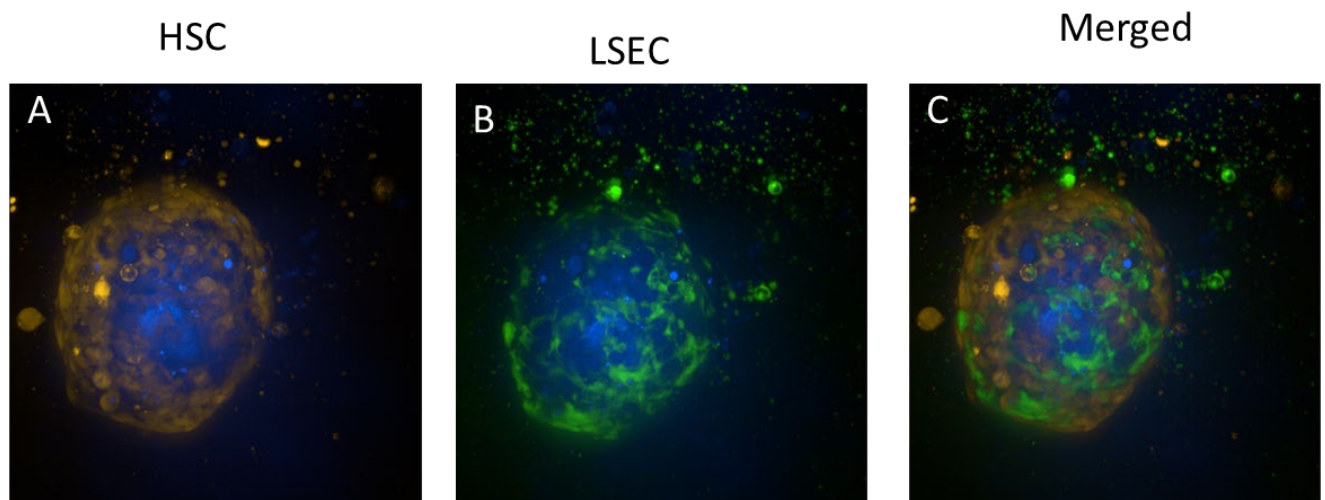


Figure 2: Representative fluorescent images of hepatocytes, LSEC and HSC in co-culture after 72 h in 20% FBS spheroid formation media. Panels A and C show the autofluorescence of the live hepatocytes (blue) and the Celltracker Orange stained HSCs (orange). Panels B and C show the autofluorescence of the live hepatocytes (blue) and the Celltracker Green stained LSECs (green). The NPCs were stained before plating. Imaged with HCl 20x water objective lens, maximum projection of a stack of 45 planes spanning 160 μm . Spheroids are approximately 200 μm in diameter.

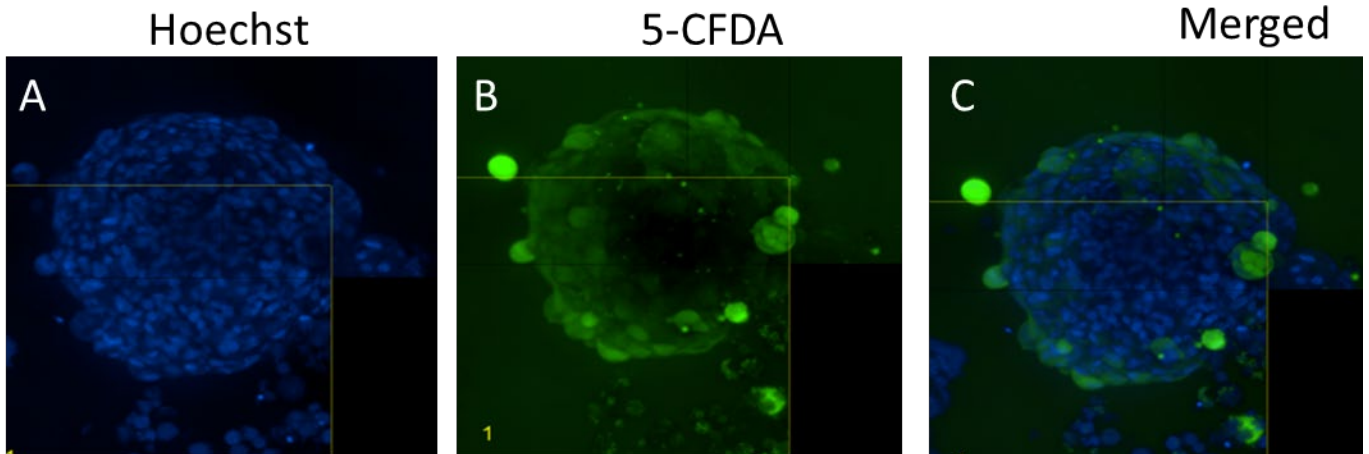


Figure 3: Spheroids formed in ultra-low attachment 96-well plates using hepatocytes with LSECs and HSCs as co-culture after 3 days were stained with 5-CFDA which is used to visualize formation of bile canaliculi, (green) and Hoechst (blue). Imaged with HCI 20x air objective lens, maximum projection of a stack of 45 planes spanning 160 μm . Spheroids are approximately 200 μm in diameter.

Further characterization of the spheroids was done using immunofluorescence (IF) staining to determine the presence of hepatocyte markers (CYP3A4, albumin and HNF alpha), LSEC marker ACTA, and HSC marker LYVE1. The IF images in Figures 4 and 5 display the staining of these markers in mono and co-culture spheroids fixed at day 7 and 10 respectively. The staining of the co-culture spheroids was uniform on day 7 and remained stable between day 7 and 10. While there was a slight increase in ACTA and Albumin staining during this time, the overall expression patterns suggest that the co-culture spheroids are already formed and functional at day 7. In contrast, the staining was not present throughout the mono-culture spheroids on day 7 and but became more uniform by day 10. This suggests that the mono-culture spheroids were still in the process of becoming more organized and functional between day 7 and 10. As expected, the expression of the LSEC and HSC markers was much lower in the mono-culture spheroids as compared to co-culture for both timepoints. As shown in Figure 6, quantitative analysis of the fluorescence intensities of the day 7 images reveals a significant increase in the hepatocyte, LSEC and HSC markers in the co-culture as compared to mono-culture spheroids.

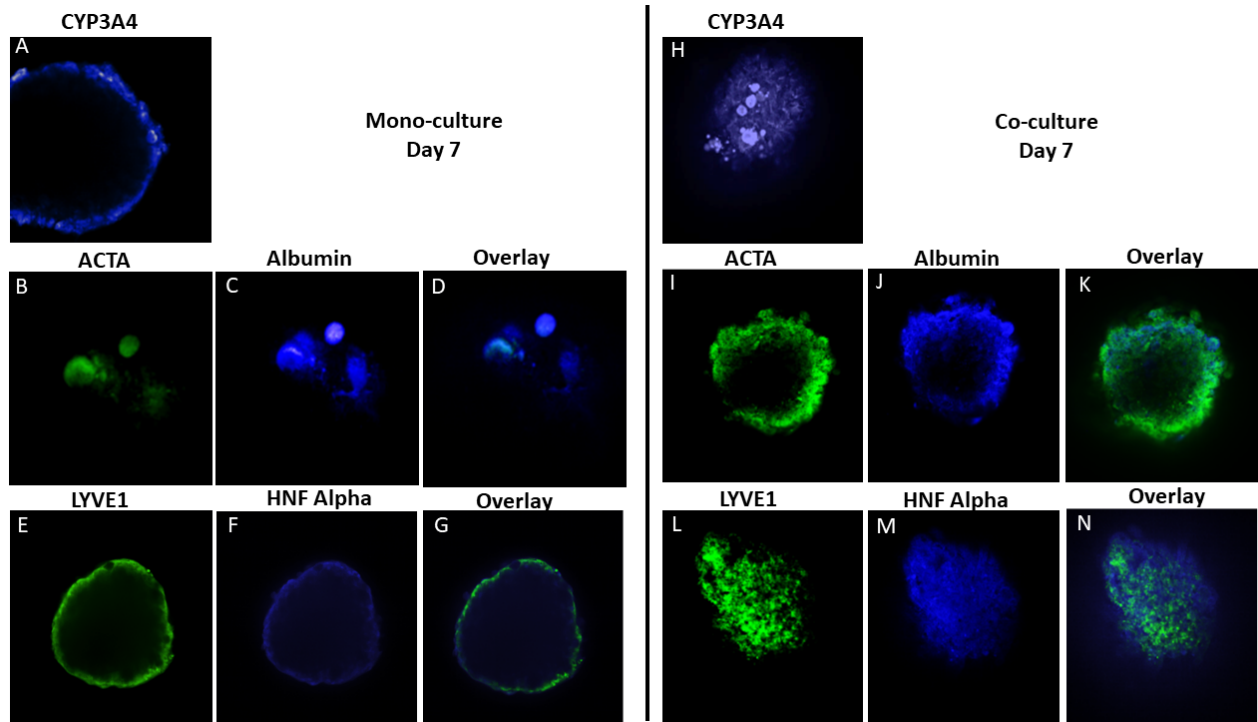


Figure 4: Immunofluorescence staining of mono and co-culture spheroids fixed at 7 days. Spheroids were stained for hepatocyte markers (CYP3A4, Albumin and HNF Alpha), LSEC marker ACTA and HSC marker LYVE1. For images B-G and I-N, each spheroid was stained with one hepatocyte marker and either an LSEC or HSC marker. In the overlay image, the blue corresponds to the hepatocyte marker and the green corresponds to either the LSEC or HSC marker. Images were taken with HCl 20x water objective lens, maximum projection of a stack of 45 planes spanning 160 μm .

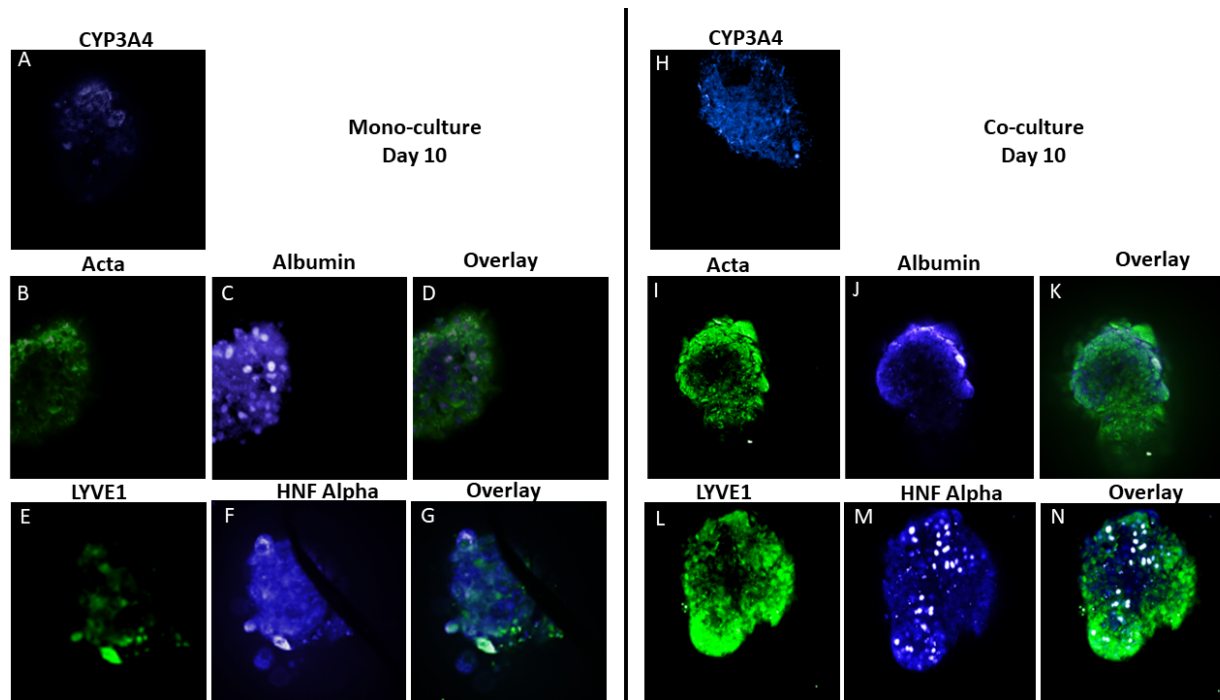


Figure 5: Immunofluorescence staining of mono and co-culture spheroids fixed at 10 days. Spheroids were stained for hepatocyte markers (CYP3A4, Albumin and HNF Alpha), LSEC marker ACTA, HSC marker LYVE1 and Kupffer cell marker CD68. For images B-G and I-N, each spheroid was stained with one hepatocyte marker and either an LSEC or HSC marker. In the overlay image, the blue corresponds to the hepatocyte marker and the green corresponds to either the LSEC or HSC marker. Images were taken with HCl 20x water objective lens, maximum projection of a stack of 45 planes spanning 160 μm .

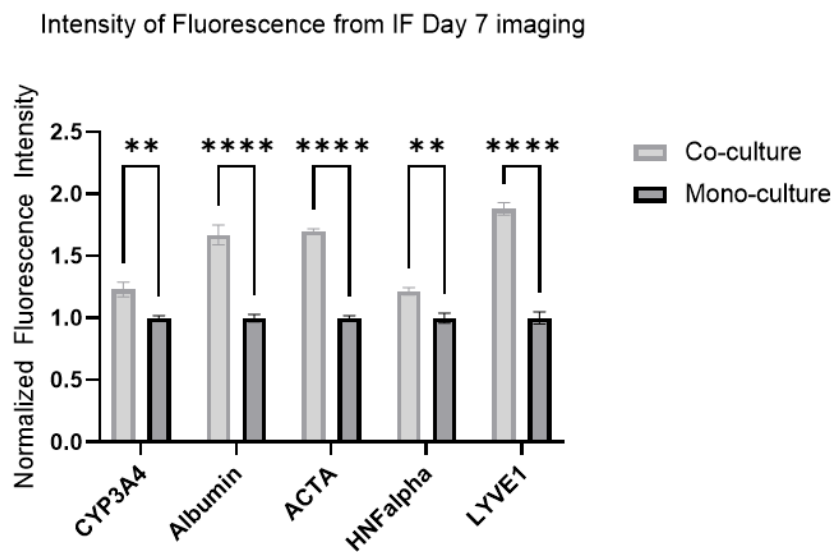


Figure 6: Quantitation of the fluorescence intensities of each antibody from the immunofluorescence day 7 images. All co-culture fluorescence intensities were normalized to the respective mono-culture intensity. ** represents $p < 0.01$, and **** represents $p < 0.0001$. Statistical significance was determined using 2-way ANOVA analysis.

Expression of cell-type specific markers was confirmed via gene expression analysis in 2D and 3D cultures. When looking at 2D cultures harvested 3 days after plating, the hepatocyte-specific genes (albumin and CYP3A4) are expressed at lower levels in hepatocyte: NPC co-cultures compared to hepatocyte mono-cultures (Figure 7A and 7B). NPC-specific genes (ACTA2 and LYVE1) are expressed at higher levels in hepatocyte: NPC co-cultures as compared to hepatocyte mono-cultures (Figure 7C and 7D).

In contrast, the gene expression of the 3D cultures could be compared over a longer period. Spheroids were harvested at day 0, 3, 7 and 10 to evaluate mRNA expression throughout the spheroid formation process. As demonstrated in Figure 8, expression of LYVE1 and ACTA were similar in mono and co-culture spheroids at day 0. As expected, a gradual increase in both NPC markers was observed on day 3, 7 and 10 in the co-culture spheroids but not in mono-culture. A substantial increase in the level of CYP3A4 was observed in the co-culture as compared to the mono-culture at all time points. This data is consistent with the IF imaging results presented in Figures 4, 5 and 6 which demonstrated a significant increase in the ACTA, LYVE1 and CYP3A4 fluorescence intensity in the co-cultures as compared to the mono-cultures. A significant improvement in the expression of CYP3A4 was observed in the 3D co-culture compared to the 2D qPCR, while the fold increase of LYVE1 and ACTA expression was lower after normalizing to the mono-culture. Albumin expression was slightly recovered in 3D co-culture compared to 2D although the expression was still lower than mono-culture in both cases. Moreover, when comparing the 2D and 3D co-cultures after normalizing to their respective monocultures, the 2D had higher expression of NPC markers while the 3D had higher expression of CYP3A4 and Albumin.

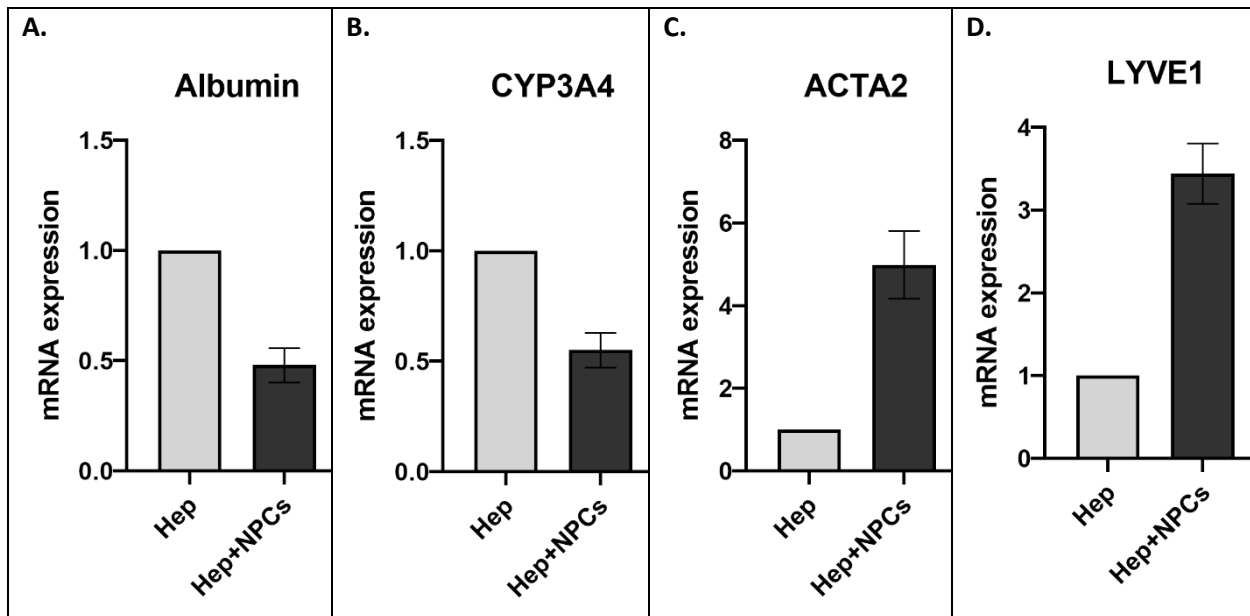


Figure 7: mRNA expression of hepatocyte and NPCs (LSECs and HSCs) specific genes in 2D hepatocyte mono-culture and hepatocytes enriched with NPCs. This figure shows the relative mRNA expression of various hepatocyte and NPC-specific genes expressed in a) hepatocyte mono-culture b) Hep: NPC co-culture. Fold change in mRNA expression over control (hepatocyte mono-culture) is calculated for each gene by normalizing the expression to the average of three housekeeping genes, GAPDH, 18s and β -actin. Grey bar indicates hepatocyte and black filled bar indicates hepatocyte and NPCs.

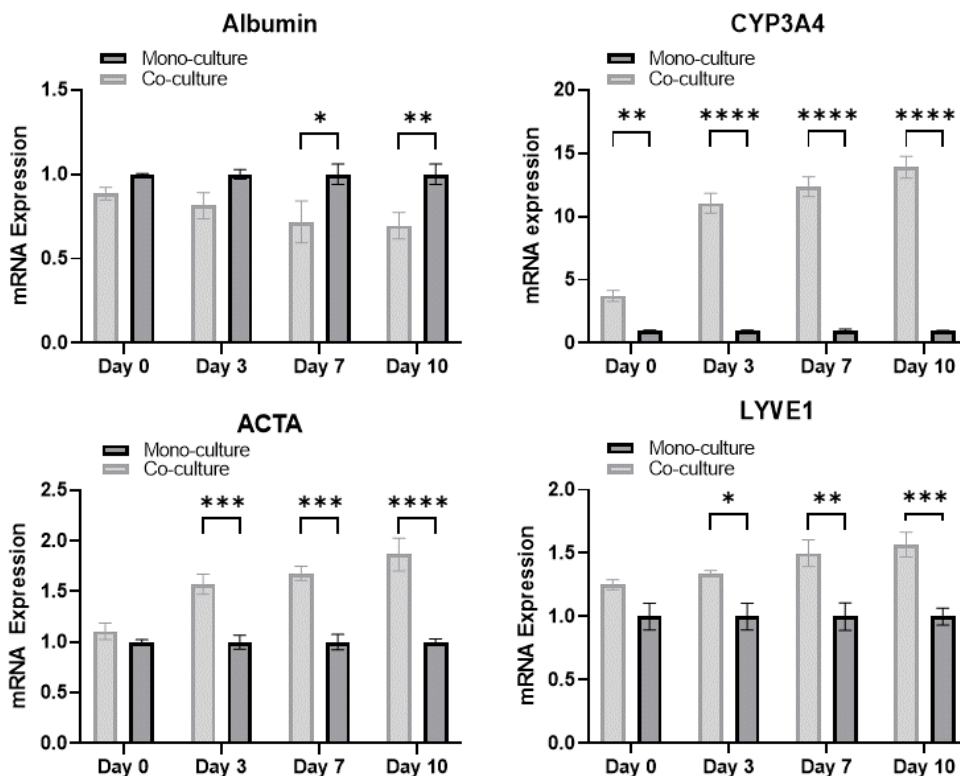


Figure 8: mRNA expression of hepatocyte markers (Albumin, CYP3A4), LSEC marker Acta, HSC marker LYVE1 determined from RT-qPCR. All co-culture samples were normalized to the respective mono-culture samples. Fold change in mRNA expression was calculated by normalizing the expression to the average of two housekeeping genes GAPDH and β -Actin. * represents $p < 0.05$, ** represents $p < 0.01$, *** represents $p < 0.001$, **** represents $p < 0.0001$. Statistical significance was determined using 2way ANOVA analysis.

12-compound screen in the 2D and 3D human in vitro liver mono-culture and co-culture model

In our study, we exposed hepatic mono- and co-cultures to various doses of test compounds under the same experimental conditions (Supplemental Figures 3 and 4). In the 2D and 3D model, we observed that human hepatocytes plated as mono-cultures produce more variable cultures. The presence of NPCs (LSECs and HSCs) in co-cultures results in a more reliable model with consistent and reproducible results. This is especially evident in 2D when looking at our CellTox Green cytotoxicity assay results, where dead cell counts obtained from mono-cultures show high standard deviation. In comparison, the co-culture model consistently shows reproducible dose–response effects of test compounds across endpoint assays with minimal variation among replicates. Detailed examination of the 2D high content imaging (HCI) data provided additional qualitative measures of cell health and properties of the test compounds. The HCI dead cell count had a strong correlation with the CellTiter-Glo viability assay dose–response curves for all compounds. By multiplexing the CellTiter-Glo viability assay and dead cell counts by HCI analysis, we get a more complete picture of the dose–response effect of the compounds.

In contrast to the 2D data, the 3D viability data was overall more variable, and the dose response curves were left shifted because of the longer treatment time. This shift resulted in some compounds having an immediate drop in viability at the lowest tested concentration in the 3D mono-culture. In addition, some compounds that did not show enough toxicity to fit a dose response curve in the 2D experiments did have toxicity in 3D with the increased treatment time.

Furthermore, we observed that some compounds caused a reproducible dose-dependent increase in viability in mono-cultures, but not in co-cultures, at sub-cytotoxic concentrations, according to the CellTiter-Glo Viability Assay in both 2D and 3D. We do not have an explanation for these observations. However, these results demonstrate the value of combining multiple endpoint assays to gain a more complete understanding of compound-induced effects.

The IC50 and EC50 values of the compounds in 2D and the IC50 values in 3D are shown in Tables 1 and 2 respectively. Because of the variability in the LDH-Glo assay for 3D cytotoxicity, we used only the CellTiter-Glo data to calculate IC50 values. We were not able to calculate IC50 or EC50 values using simple model-fitting analysis for compounds that showed minimal toxicity. Sucrose served as a negative control compound and showed no cytotoxicity or loss of viability in mono- and co-cultures.

Table 1. IC50 and EC50 values for test compounds after treatment of 2D mono- and co-cultures

Compound	IC50 values based on viability using CellTiter-Glo Viability Assay		EC50 values based on cytotoxicity using dead cell counts by HCl technique	
	Mono-culture	Co-culture	Mono-culture	Co-culture
Tamoxifen	36.36 μ M	40.03 μ M	37.07 μ M	36.98 μ M
Bisphenol A	384.0 μ M	414.2 μ M	349.1 μ M	356.1 μ M
Acetaminophen	32.26 mM	29.98 mM	127.9 mM	56.03 mM
Acetochlor	81.85 μ M	79.62 μ M	77.20 μ M	82.34 μ M
Triflumizole	310.5 μ M	347.5 μ M	368.7 μ M	376.8 μ M
Dimethenamid	134.9 μ M	131.9 μ M	114.2 μ M	130.6 μ M
Ethofumesate	124.8 μ M	686 μ M	866.2 μ M	389.7 μ M

Table 2. IC50 values for test compounds after treatment of 3D mono- and co-cultures

Compound	IC50 values based on viability using CellTiter-Glo 3D Viability Assay	
	Mono-culture	Co-culture
Tamoxifen	28.99 μ M	22.25 μ M
Bisphenol A	297.7 μ M	231.5 μ M
Acetaminophen	14.83 mM	6.859 mM
Acetochlor	3.378 μ M	52.76 μ M
Triflumizole	280.6 μ M	213.9 μ M
Dimethenamid	4.277 μ M	57.99 μ M
Ethofumesate	323.5 μ M	403.7 μ M
Aflatoxin B1	1.442 μ M	21.85 μ M
Ametryn	N/A	877.8 μ M

In the 2D, except for acetaminophen and ethofumesate, there is little difference in toxicity between mono- and co-cultures. The presence of NPCs, while providing a more stable culture model does not significantly affect cellular toxicity.

In the 3D there were differences in toxicity between mono- and co- cultures for several compounds. Mono-cultures had increased cytotoxicity to acetochlor, dimethenamid and aflatoxin while co-cultures had increased cytotoxicity to acetaminophen and ametryn. Monocultures displayed a statistically significant ($p < 0.0001$) decrease in viability at all tested concentrations of acetochlor, dimethenamid and aflatoxin. In contrast, co-cultures displayed a statistically significant ($p < 0.001$) decrease in viability when treated with concentrations $\geq 316 \mu$ M of ametryn and ≥ 8.9 mM acetaminophen.

Despite the complexity and increased compound treatment time gained by use of the 3D cell culture, in most cases results were very similar to those in 2D culture. Comparable cytotoxicity values were acquired for most compounds. However, there were two notable differences. There was no toxicity to aflatoxin B1 in 2D cell culture, but there was in 3D. Additionally, there was no ametryn toxicity in 2D while we did observe cytotoxicity in 3D co-culture.

QIVIVE

For the compounds that we were able to obtain IC50 or EC50 values in 2D and 3D, QIVIVE analysis was performed to determine a human equivalent dose (HED) as shown in Tables 3 and 4.

Table 3. QIVIVE values derived from IC50 values for test compounds after treatment of 2D mono- and co-cultures

Compound	Human Equivalent Dose (HED) IVIVE values based on viability using CellTiter-Glo Viability Assay (mg/kg-day)	
	Mono- culture	Co-culture
Tamoxifen	0.16	0.17
Bisphenol A	212.06	228.74
Acetaminophen	45170.2	41977.74
Acetochlor	377.82	367.52
Triflumizole	68.21	76.34
Dimethenamid	374.24	365.92
Ethofumesate	217.15	1193.63

Table 4. QIVIVE values derived from IC50 values for test compounds after treatment of 3D mono- and co-cultures

Compound	Human Equivalent Dose (HED) IVIVE values based on viability using CellTiter-Glo 3D Viability Assay (mg/kg-day)	
	Mono-culture	Co-culture
Tamoxifen	0.12	0.10
Bisphenol A	164.40	127.85
Acetaminophen	20764.84	9603.91
Acetochlor	15.59	243.54
Triflumizole	61.64	46.99
Dimethenamid	11.87	160.88
Ethofumesate	562.88	702.43
Aflatoxin B1	2.09	31.70
Ametryn	N/A	100.95

While LD50 values for these compounds in humans are not available, we can calculate HED values from LD50 values for rat from the EPA's CompTox Chemicals Dashboard¹³ (Table 5) using previously published methods.¹⁴ Comparing the HED values, we obtained similar values for bisphenol A, acetochlor, and triflumizole for both 2D and 3D. There is some variability in the ethofumesate data for 2D, but with the exception of the monoculture viability data the other values are comparable. In both 2D and 3D HED values for tamoxifen were low and acetaminophen were high. Our HED of tamoxifen in all culture models and assays was calculated to be 0.16 mg/kg-day. For an average 70 kg person this would be 11 mg of tamoxifen per day. However, the therapeutic tamoxifen dose for an ovarian cancer patient is 40 mg/day.¹⁵ For acetaminophen, a compound that undergoes extensive metabolism, this might reflect the in vitro to in vivo differences.¹⁶ In humans acute lethal acetaminophen dose is >12 g, while elevated serum alanine aminotransferase levels are observed with a 4 g daily dose.^{16,17} Based on our IC50s, the daily acute HED for acetaminophen in a 70 kg person would range from 3,000 g – 13,000 g. Comparing these HED values with the calculated HED values in Table 6, we see some agreement for ethofumesate and ametryn. For aflatoxin B1 in 3D culture, the monoculture data was consistent with previous values, but the co-culture value was significantly higher.

Table 5. Rat LD50 values from EPA's CompTox Chemicals Dashboard and Calculated HED values

Compound	LD50 (mg/kg-day)	Calculated HED (mg/kg-day)
Tamoxifen	4100	664
Bisphenol A	2000	324
Acetaminophen	1940	314
Acetochlor	763	124
Triflumizole	715	116
Dimethenamid	371	60
Ethofumesate	6400	1037
Aflatoxin B1	4.8	0.78
Ametryn	1630	264

Conclusions

In vitro hepatotoxicity models range in complexity from 2D cell culture to liver-on-a chip.⁶ While pharmaceutical screening for Drug Induced Liver Injury (DILI) has long been a focus of research, little work has been done to develop physiologically relevant hepatotoxicity screening models for commodity and specialty chemicals. We have functionally characterized and evaluated two different 2D models and two different 3D cell culture models, using either hepatocytes alone or hepatocytes co-cultured with NPCs. In our study the 2D and 3D models that were solely hepatocytes resulted in higher levels of albumin, compared to their counterparts that included NPCs. However, in 3D spheroids, CYP3A4 levels were much higher in co-culture than mono-culture, compared to the 2D culture with lower CYP3A4 levels in co-culture than mono-culture. This variability has also been observed in other hepatocyte co-culture systems.⁵

Using various cell tracker dyes, we have confirmed the presence of all cell types in our co-culture models, their spatial orientation and polarity within the spheroids. Interestingly, we have found hepatocytes forming the core of the 3D spheroid, with the NPCs creating an exterior “cage” around these hepatocytes. Previous 2D studies have looked at how the location of NPCs affects albumin and

CYP production, and the higher level of CYP3A4 in our co-culture 3D spheroid might be due to the spatial arrangement of hepatocytes and NPCs.¹⁸

Despite the increased complexity and presence of the bile canicular network in the 3D co-culture model, the IC₅₀ cytotoxicity responses of the mono- and co- 2D and 3D cultures to the panel of test compounds were very similar. However, in either case the presence of NPCs provided a cytotoxicity model with less variability than monoculture. The HED values obtained by IVIVE analysis for the non-pharmaceutical compounds were consistent with previously obtained in vivo data. While larger scale validation studies need to be performed, the less complex 2D hepatocyte co-culture model could be a viable high-throughput method for screening hepatotoxicity.

Acknowledgements

Funding for this study was provided by the American Chemistry Council Long Range Research Initiative (contract 3005). We thank Aarati Ranade and Pradeep Kumar for their assistance in data acquisition.

References

1. McMullen PD, Andersen ME, Cholewa B, et al. Evaluating opportunities for advancing the use of alternative methods in risk assessment through the development of fit-for-purpose in vitro assays. *Toxicol In Vitro*. Apr 2018;48:310-317. doi:10.1016/j.tiv.2018.01.027
2. Martignoni M, Groothuis GM, de Kanter R. Species differences between mouse, rat, dog, monkey and human CYP-mediated drug metabolism, inhibition and induction. *Expert Opin Drug Metab Toxicol*. Dec 2006;2(6):875-94. doi:10.1517/17425255.2.6.875
3. Olson H, Betton G, Robinson D, et al. Concordance of the toxicity of pharmaceuticals in humans and in animals. *Regul Toxicol Pharmacol*. Aug 2000;32(1):56-67. doi:10.1006/rtph.2000.1399
4. Proctor WR, Foster AJ, Vogt J, et al. Utility of spherical human liver microtissues for prediction of clinical drug-induced liver injury. *Arch Toxicol*. Aug 2017;91(8):2849-2863. doi:10.1007/s00204-017-2002-1
5. Kammerer S. Three-Dimensional Liver Culture Systems to Maintain Primary Hepatic Properties for Toxicological Analysis In Vitro. *Int J Mol Sci*. Sep 23 2021;22(19)doi:10.3390/ijms221910214
6. Collins SD, Yuen G, Tu T, et al. In Vitro Models of the Liver: Disease Modeling, Drug Discovery and Clinical Applications. In: Tirnitz-Parker JEE, ed. *Hepatocellular Carcinoma*. 2019.
7. Gomez-Lechon MJ, Castell JV, Donato MT. Hepatocytes--the choice to investigate drug metabolism and toxicity in man: in vitro variability as a reflection of in vivo. *Chem Biol Interact*. May 20 2007;168(1):30-50. doi:10.1016/j.cbi.2006.10.013
8. Kegel V, Deharde D, Pfeiffer E, Zeilinger K, Seehofer D, Damm G. Protocol for Isolation of Primary Human Hepatocytes and Corresponding Major Populations of Non-parenchymal Liver Cells. *J Vis Exp*. Mar 30 2016;(109):e53069. doi:10.3791/53069
9. Mitra A, Mishra L, Li S. Technologies for deriving primary tumor cells for use in personalized cancer therapy. *Trends Biotechnol*. Jun 2013;31(6):347-54. doi:10.1016/j.tibtech.2013.03.006
10. Bell CC, Dankers ACA, Lauschke VM, et al. Comparison of Hepatic 2D Sandwich Cultures and 3D Spheroids for Long-term Toxicity Applications: A Multicenter Study. *Toxicological Sciences*. 2018;162(2):655-666. doi:10.1093/toxsci/kfx289
11. Livak KJ, Schmittgen TD. Analysis of relative gene expression data using real-time quantitative PCR and the 2(-Delta Delta C(T)) Method. *Methods*. Dec 2001;25(4):402-8. doi:10.1006/meth.2001.1262
12. Wetmore BA, Wambaugh JF, Allen B, et al. Incorporating High-Throughput Exposure Predictions With Dosimetry-Adjusted In Vitro Bioactivity to Inform Chemical Toxicity Testing. *Toxicol Sci*. Nov 2015;148(1):121-36. doi:10.1093/toxsci/kfv171
13. CompTox Chemicals Dashboard.

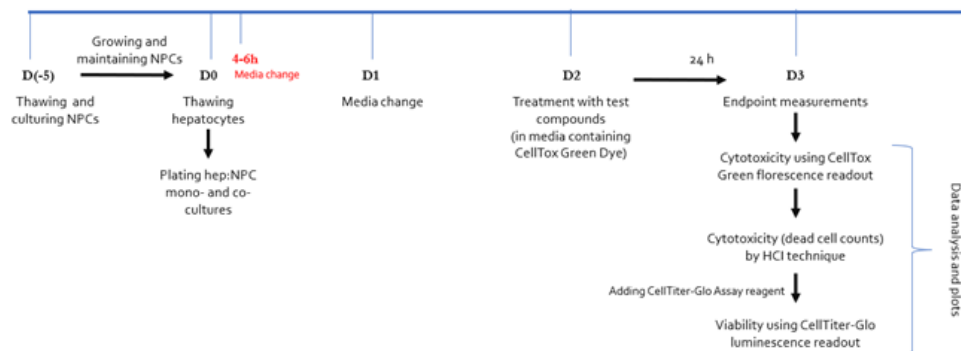
14. Nair AB, Jacob S. A simple practice guide for dose conversion between animals and human. *J Basic Clin Pharm*. Mar 2016;7(2):27-31. doi:10.4103/0976-0105.177703
15. Lindemann K, Gibbs E, Avall-Lundqvist E, et al. Chemotherapy vs tamoxifen in platinum-resistant ovarian cancer: a phase III, randomised, multicentre trial (Ovaresist). *Br J Cancer*. Feb 14 2017;116(4):455-463. doi:10.1038/bjc.2016.435
16. Mazaleuskaya LL, Sangkuhl K, Thorn CF, FitzGerald GA, Altman RB, Klein TE. PharmGKB summary: pathways of acetaminophen metabolism at the therapeutic versus toxic doses. *Pharmacogenet Genomics*. Aug 2015;25(8):416-26. doi:10.1097/FPC.0000000000000150
17. Watkins PB, Kaplowitz N, Slattery JT, et al. Aminotransferase Elevations in Healthy Adults Receiving 4 Grams of Acetaminophen DailyA Randomized Controlled Trial. *JAMA*. 2006;296(1):87-93. doi:10.1001/jama.296.1.87
18. Bale SS, Golberg I, Jindal R, et al. Long-term coculture strategies for primary hepatocytes and liver sinusoidal endothelial cells. *Tissue Eng Part C Methods*. 2015;21(4):413-422. doi:10.1089/ten.TEC.2014.0152

Supplementary Information

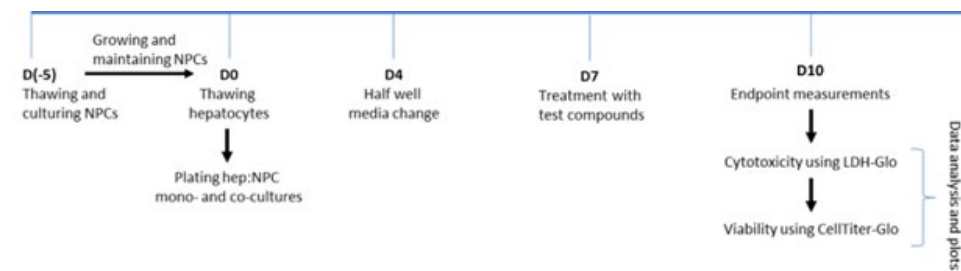
Supplementary Table 1. Compounds and concentrations tested in the 2D and 3D in vitro human model

Name of Compound	Concentration Range (mM or μM)	Compound Type
Tamoxifen (TMX)	0, 5.9, 8.8, 13.2, 19.8, 29.6, 44.4, 66.7 and 100 μM	Pharmaceutical
Bisphenol A (BPA)	0, 4.64, 10, 21.54, 46.42, 100, 215.44, 464.16 and 1000 μM	Industrial chemical
Acetaminophen (APAP) 2D	0, 1.78, 3.16, 5.62, 10, 17.8, 31.6, 56.2 and 100 mM	Pharmaceutical
Acetaminophen (APAP) 3D	0, 0.89, 1.58, 2.81, 5, 8.9, 15.8, 28.1, 50 mM	Pharmaceutical
Acetochlor	0, 10, 17.8, 31.6, 56.2, 100, 178, 316 and 562 μM	Herbicide
Triflumizole	0, 0.316, 1, 3.16, 10, 31.6, 100, 316 and 1000 μM	Fungicide
Aflatoxin B1 2D	0, 0.89, 1.58, 2.81, 5, 8.81, 15.8, 28.1 and 50 μM	Food contaminant
Aflatoxin B1 3D	0, 0.445, 0.79, 1.405, 2.5, 4.445, 7.9, 14.05, 25 μM	Food contaminant
Ametryn	0, 17.8, 31.6, 56.2, 100, 178, 316, 562 and 1000 μM	Herbicide
Dimethenamid	0, 3.56, 6.32, 11.3, 20, 35.6, 63.3, 112 and 200 μM	Herbicide
Carbaryl	0, 0.063, 0.2, 0.63, 2, 6.32, 20 and 63.2 μM , and 200 μM	Insecticide
Flusilazole	0, 0.46, 1, 2.15, 4.64, 10, 21.54, 46.42 and 100 μM	Fungicide
Ethofumesate	0, 0.316, 1, 3.16, 10, 31.6, 100, 316 and 1000 μM	Herbicide
Sucrose	0, 1.78, 3.16, 5.62, 10, 17.78, 31.6, 56.2 and 100 mM	Negative Control

Supplementary Figure 1: Schematic of experimental design (plating, treatment, and data collection) for testing compounds in hepatocyte: NPC 2D mono- and co-cultures



Supplementary Figure 2: Schematic of experimental design (plating, treatment, and data collection) for testing compounds in hepatocyte-NPC 3D mono- and co-cultures



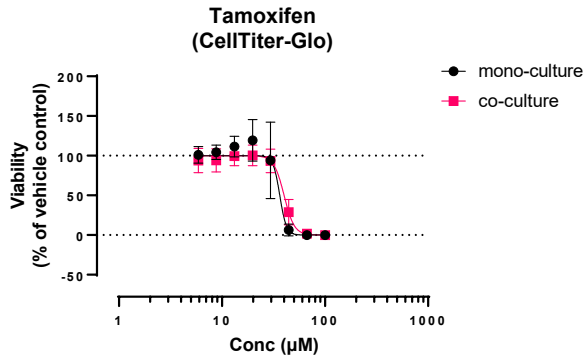
Supplementary Table 2: Media used for thawing, plating, and maintenance of hepatocytes, LSECs, and HSCs

Media	Vendor/Catalog #	Component A	Component B
Hepatocyte thawing media	Lonza MCAT50	Ready to use	—
Hepatocytes plating media	Lonza MP100	MP100-1	MP100-2
Hepatocyte culture media (HCM)	Lonza CC-319	HBM basal medium (CC-3199)	SingleQuot™ kit (CC-4182); ascorbic acid, bovine serum albumin, hydrocortisone, human epidermal growth factor, transferrin, insulin, and gentamycin/amphotericin B
DMEM+ media (for LSECs and HSCs)	Invitrogen 11965118	DMEM	20% FBS
50/50 media (HCM DMEM+)		HCM	DMEM+

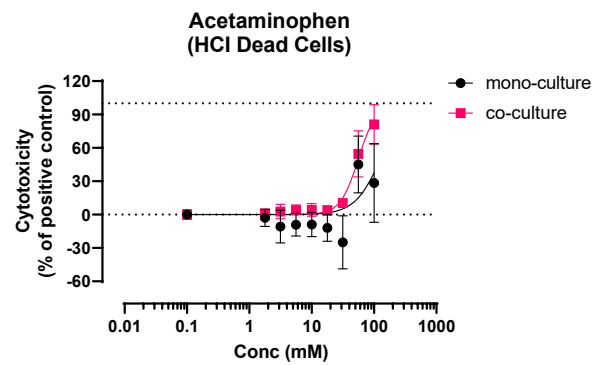
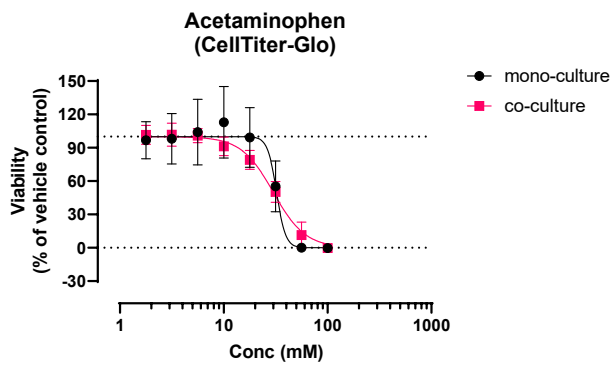
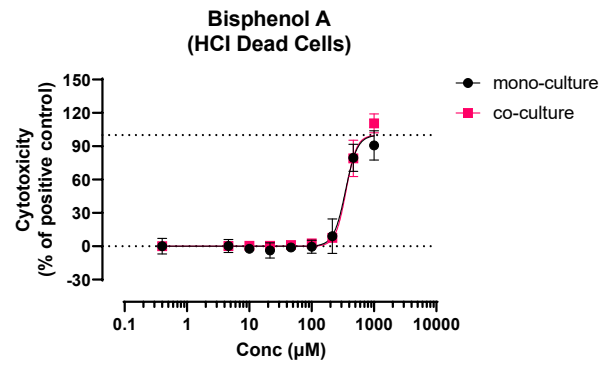
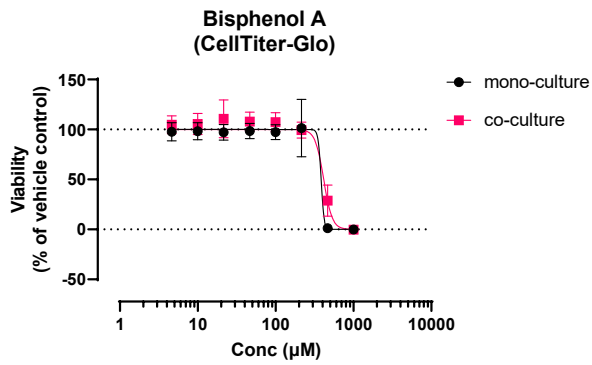
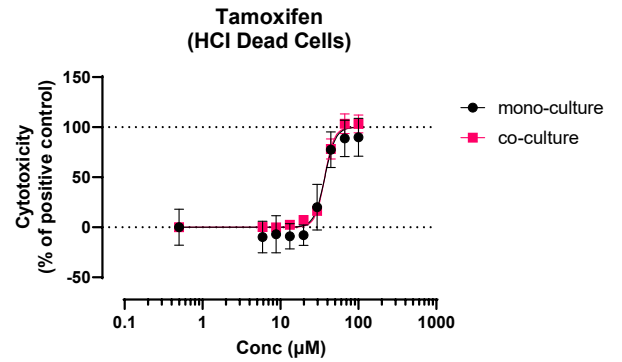
Supplementary Table 3. Primers used in qPCR

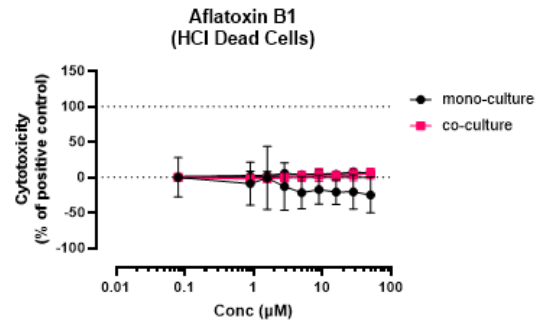
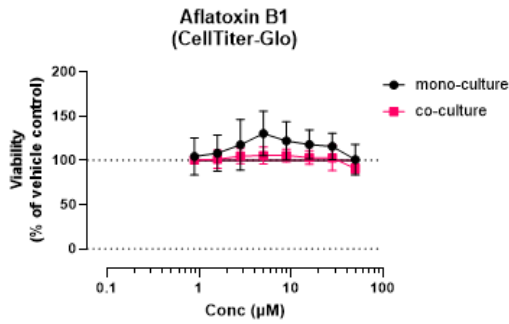
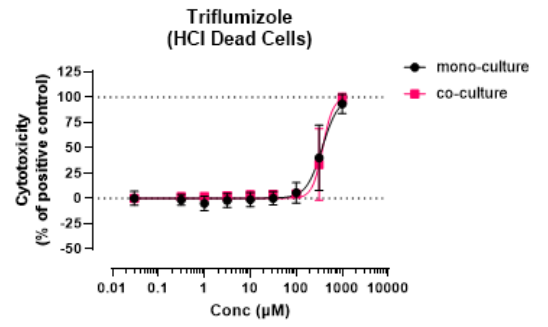
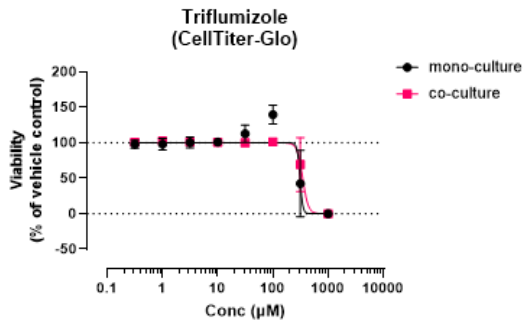
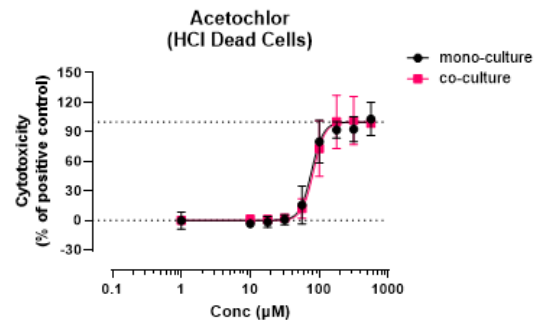
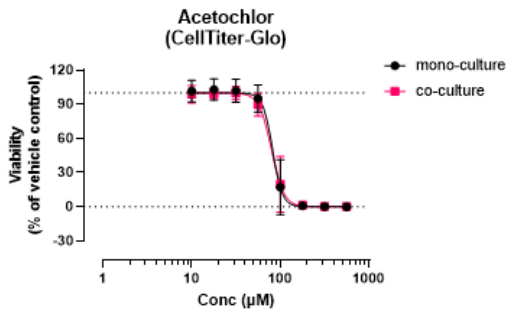
Gene (Human)		Sequence (5' -> 3')
ACTA	Forward	CTATGCCTCTGGACGCACAAC
	Reverse	CAGATCCAGACGCATGATGGCA
Albumin	Forward	GATGAGATGCCTGCTGACTTGC
	Reverse	CACGACAGAGTAATCAGGATGCC
β-actin	Forward	CATGTACGTTGCTATCCAGGC
	Reverse	CTCCTTAATGTCACGCACGAT
CD68	Forward	CGAGCATCATTCTTTACCAGCT
	Reverse	ATGAGAGGCAGCAAGATGGACC
CYP3A4	Forward	GTGGGGCTTTTATGATGGTCA
	Reverse	GCCTCAGATTTCTCACCAACACA
GAPDH	Forward	ACAACCTTGGTATCGTGAAGG
	Reverse	GCCATCACGCCACAGTTTC
LYVE1	Forward	TGTTCCCTGGCTCTGAAGG
	Reverse	CTGGATGGAAAGCTCTTCTGC

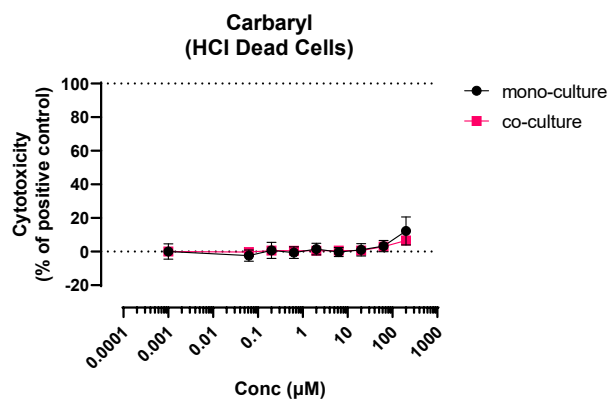
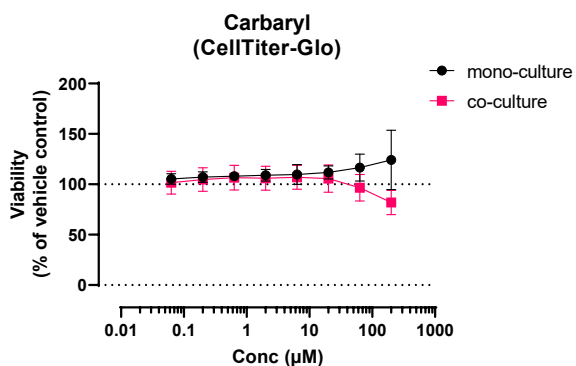
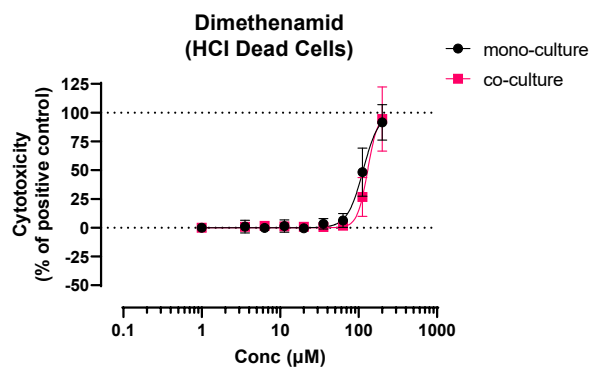
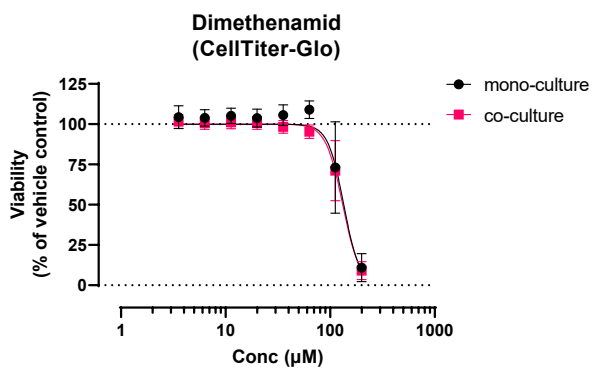
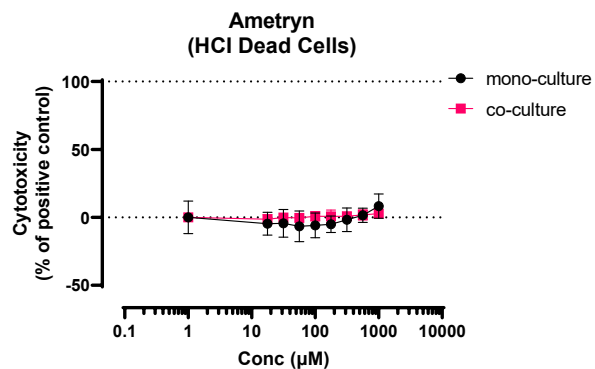
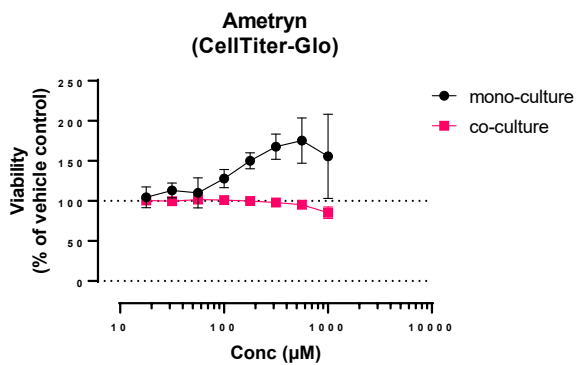
A

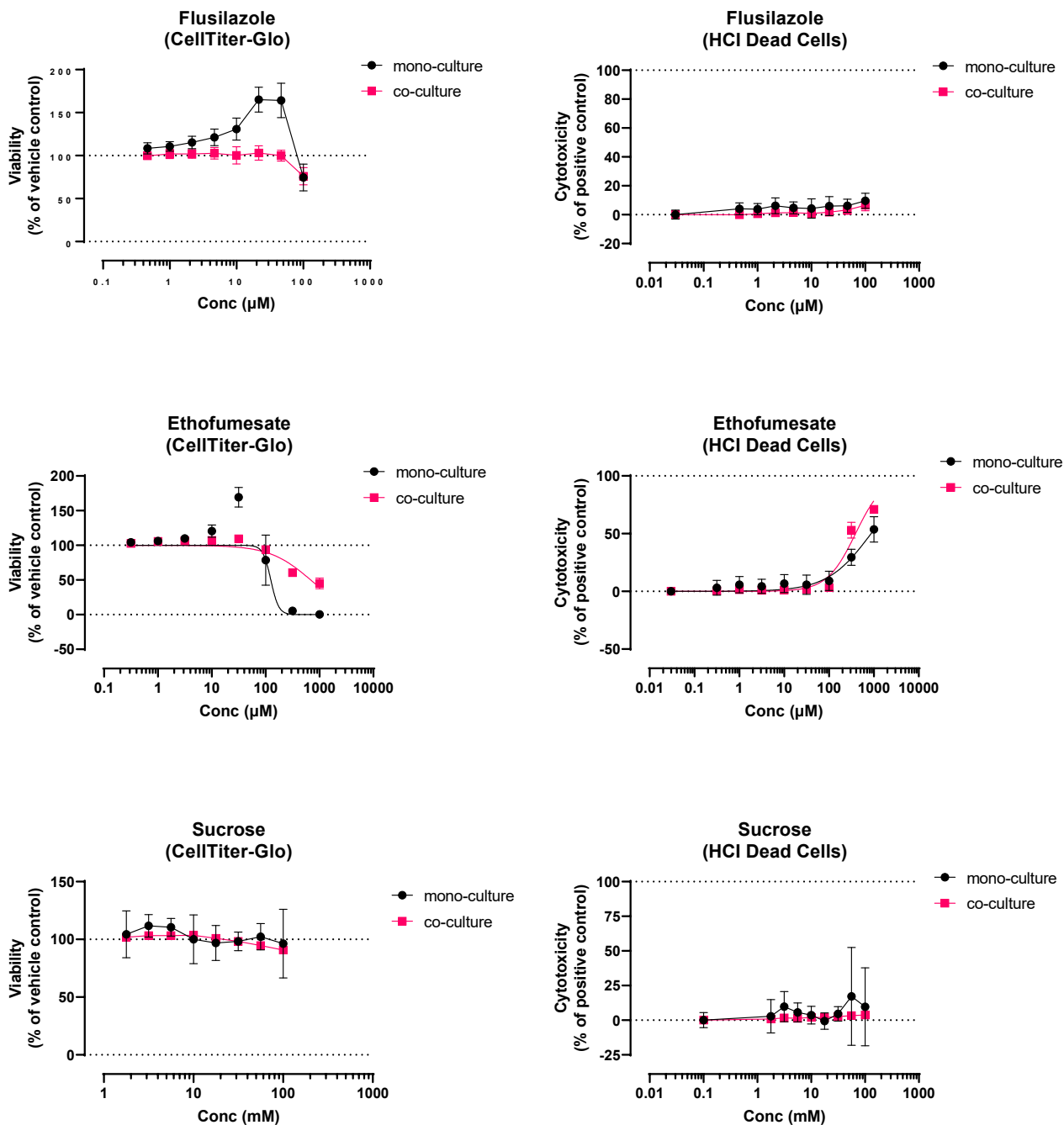


B



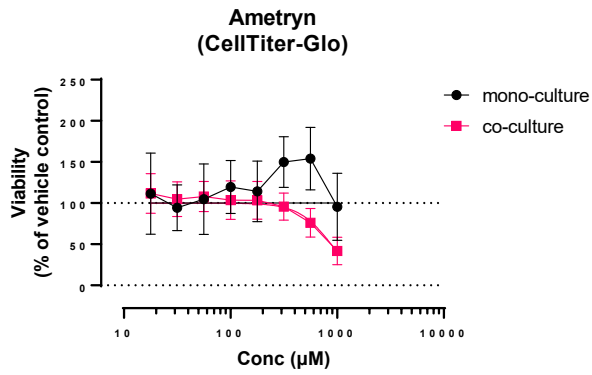




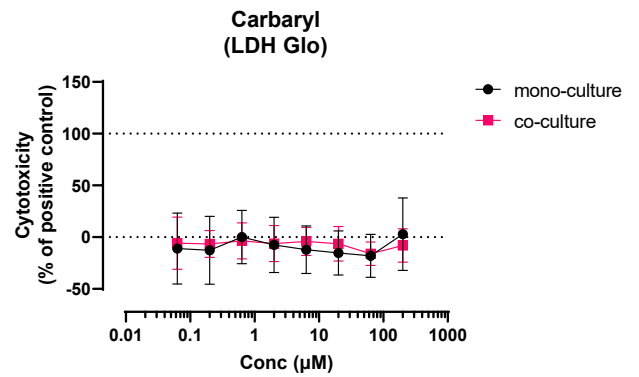
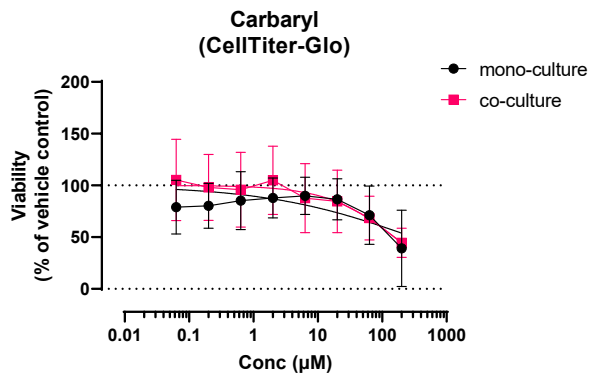
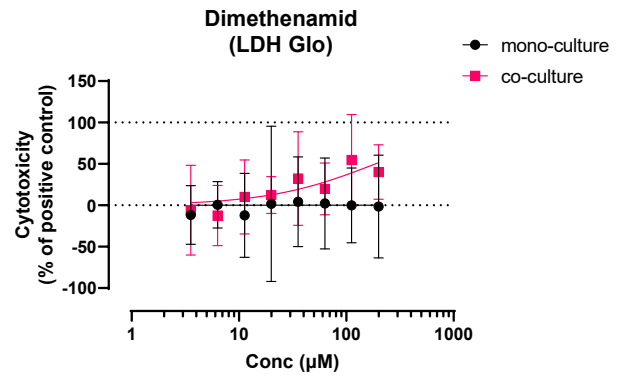
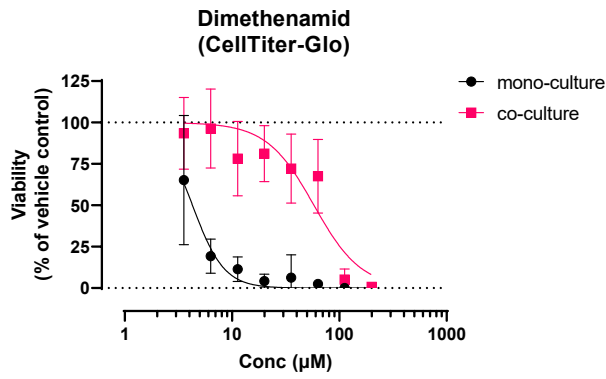
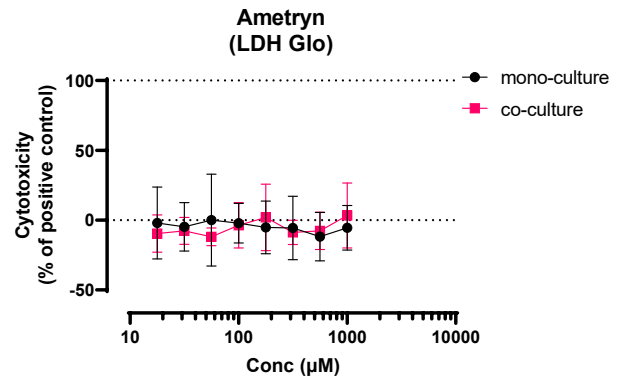


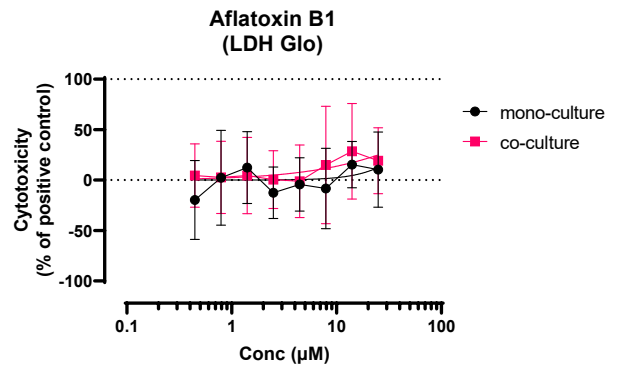
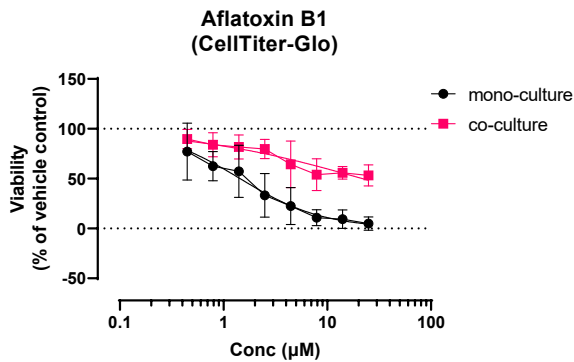
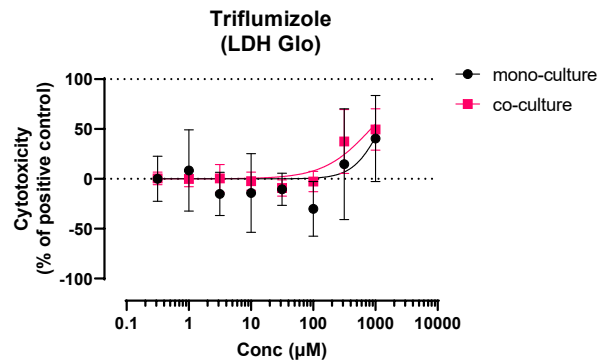
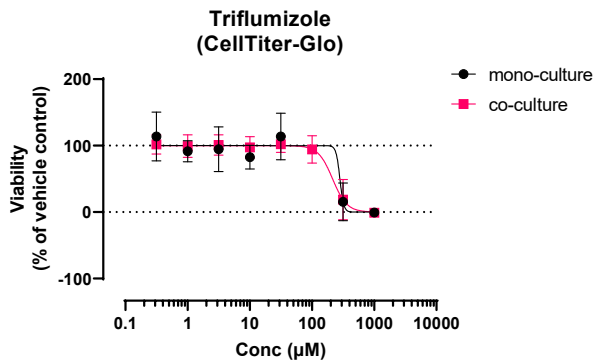
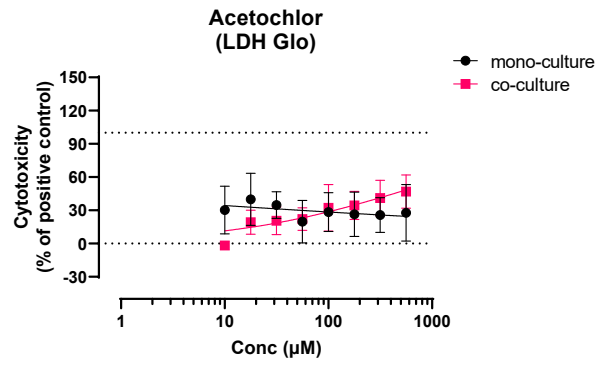
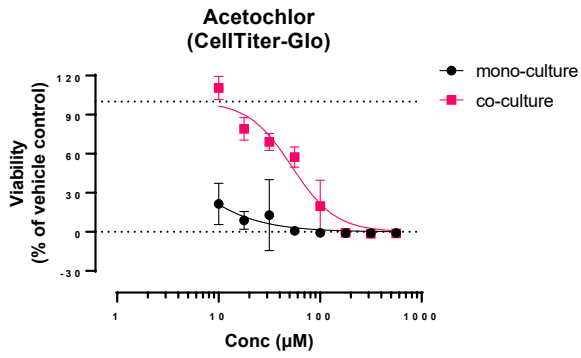
Supplementary Figure 3: Dose–response curves for 12 test compounds in hepatic 2D mono- and co-cultures. Response is viability measured using CellTiter-Glo Viability (panel A) and cytotoxicity measurement by counting number of dead cells using HCl technique (panel B). Each value represents the mean and SD of measurements obtained from multiple biological replicate experiments (N=3).

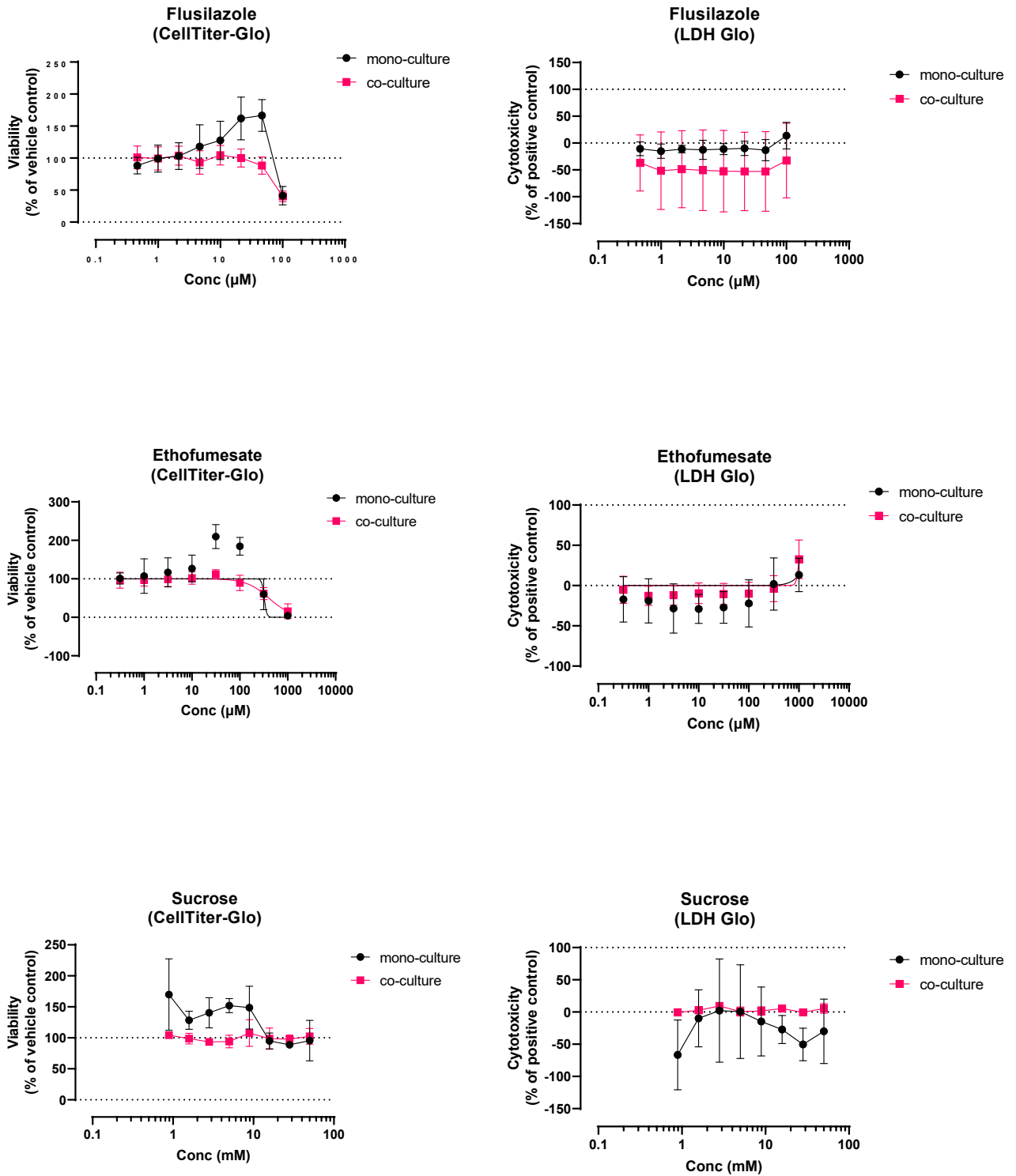
A



B







Supplementary Figure 4: Dose–response curves for 12 test compounds in hepatic 3D mono- and co-cultures. Response is viability measured using CellTiter-Glo 3D (panel A) and cytotoxicity using LDH-Glo (panel B). Each value represents the mean and SD of measurements obtained from multiple biological replicate experiments (N=3).